Front. Earth Sci. 2015, 9(4): 683–690
DOI 10.1007/s11707-015-0537-0

RESEARCH ARTICLE

Observational evidence for atmospheric modulation of the Loop Current migrations

D. Lindo-Atichati (✉)[1], P. Sangrà[2]

1 Department of Engineering Science & Physics, College of Staten Island, City University of New York, Staten Island, NY 10314, USA
2 Instituto de Oceanografía y Cambio Global (IOCAG), Universidad de Las Palmas de Gran Canaria, Las Palmas de Gran Canaria, Spain

Abstract Recent modeling studies on the shedding of Loop Current rings suggest that the intensification of the dominant zonal wind field delays the detachment of rings and affects the Loop Current migrations. The atmospheric modulation of the Loop Current migrations is analyzed here using reanalysis winds and altimetry-derived observations. A newly developed methodology is applied to locate the Loop Current front, and a wavelet-based semblance analysis is used to explore correlations with atmospheric forcing. The results show that weakening (intensification) of the zonal wind stress in the eastern Gulf of Mexico is related with the Loop Current excursions to the north (south). Semblance analyses confirm negative correlations between the zonal wind stress and the Loop Current migrations during the past 20 years. The intrusions of the Loop Current might involve an increase of the Yucatan Transport, which would balance the westward Rossby wave speed of a growing loop and delay the ring shedding. The results of this study have consequences for the interpretation of the chaotic processes of ring detachment and Loop Current intrusions, which might be modulated by wind stress.

Keywords Loop Current, wind stress, wavelet analysis, altimetry, air-sea interactions, Gulf of Mexico

1 Introduction

The wind regime in the Caribbean is governed by the North Atlantic subtropical high. Located between Bermuda and the Azores, the high air pressure zone centered at around 30°N drives north-easterly trade winds on the southern side of its clockwise atmospheric circulation all year round (Tomczak and Godfrey, 2003). The winds over the Caribbean Sea vary owing to the northward migration of the Intertropical Convergence Zone (Muñoz et al., 2008), from its southernmost position in winter (over the Amazon basin and centred at the Equator) to its northernmost position in summer (over Costa Rica and centred at 11°N) (Poveda et al., 2006). Once they approach the Yucatan basin the north-easterly trade winds intensify, forming the easterly Caribbean low-level jet (12.5°N–17.5°N; 70°W–80°W) with wind speeds larger than 13 $m \cdot s^{-1}$ (Wang, 2007; Wang and Lee, 2007).

In the Gulf of Mexico (GoM), a good understanding of the oceanographic conditions of Loop Current (LC) system is important for coastal ecosystems, society, and the economy as evidenced by the Deepwater Horizon oil spill (Smith et al., 2014). Significant insights into the dynamics of the LC and ring shedding are given by the findings of Hurlburt and Thompson (1980), Pichevin and Nof (1997), and Nof (2005). In particular, the latter explains how the LC bifurcates into a steady branch that does turn eastward and an unsteady branch that periodically sheds eddies westward. Their works indicate that if we fully understand mass balances in the GoM we can also understand the dynamics of LC migrations and ring detachments.

The research presented here regarding the correlation and possible effects of atmospheric pressure and wind forcing on the meridional migrations (northward and southward excursions) of the LC has been inspired by the recent modeling work of Chang and Oey (2010, 2013a, b). They show that the intensification of the prevailing zonal wind field creates an eastward transport in the central GoM that delays the detachment of rings and strengthens them. This delay in the ring shedding is caused by the variability in Ekman transport instead of lineal Ekman pumping, since wind curl is excluded in their study. Because the ring shedding process is generated to balance the momentum flux of the steady current that turns eastward (Pichevin and Nof, 1997; Nof, 2005), the detachment of LC rings is

Received March 26, 2015; accepted June 8, 2015

E-mail: David.LindoAtichati@csi.cuny.edu

closely related with the LC migrations. Specifically, when there is intensification in the Yucatan Current, the continued influx of Yucatan transport makes the LC grow (Nof, 2005; Chang and Oey, 2013b). Although a comprehensive observational study on the background long-term variability of surface oceanographic conditions has been recently conducted in the offshore GoM (Muller-Karger et al., 2014), to date the local atmospheric control of the LC migrations has not been investigated utilizing an observational approach. The aim of the present work is to shed light on the local atmospheric modulation of LC migrations between 1993 and 2012. Here we use altimetry observations and wind field data to test the hypotheses that (i) sea level pressure and (ii) wind stress are anticorrelated with the LC migrations.

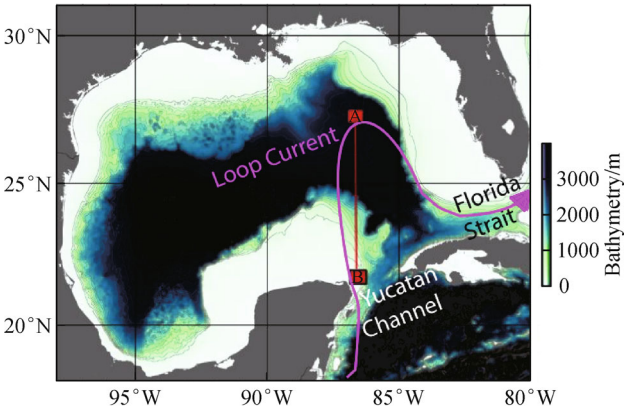

Fig. 1 Bottom topography of the Gulf of Mexico. Data retrieved from ETOPO1 1-minute Global Relief. The map illustrates the section A–B used to estimate differences in mean sea level pressure and differences in mean wind stress. Main geographical features and generalized flow of the Loop Current are marked.

2 Data and methods

To explore whether variability of Ekman transport has some effect on the migrations of the LC, the monthly atmospheric boundary-layer sea level pressure gradient (SLPG) between the northern and southern locations of the LC is calculated from January 1993 to December 2012. This time series is compared with the time series of the LC migrations for the same period of time. There are several reasons why SLPG is used here as a first metric to compare the variability of Ekman transport with the LC migrations. First, SLPG is a parameter easy to measure and reflects the fluctuations in the difference of atmospheric pressure at sea level between two relevant locations. Here our relevant locations are the northeastern and southeastern GoM where the LC oscillates. Second, SLPG can be easily used as an index of the variability in the predominantly zonal (westward) wind field in the region. Third, to the best of our knowledge there is no index similar to the North Atlantic Oscillation index specific of the GoM. After this first examination of LC migrations and SLPG, we extend the analysis to the LC migrations and the wind stress variability, which ultimately drives Ekman transport.

Monthly means of surface winds are computed from the 6-hourly wind fields reanalysis delivered by the U.S. Navy Fleet Numerical Meteorology and Oceanography Center on a 1° horizontal resolution, and posted to the Pacific Fisheries Environmental Laboratory Live Access Server (Clancy, 1992). Monthly mean pressure differences between the northeastern and southeastern locations in the GoM are estimated. The northeastern and southeastern locations are located along longitude 86.5°W at latitudes 27.5°N and 21.5°N, one degree of latitude above the mean northernmost location of the LC (Lindo-Atichati et al., 2013) and in the middle of the Yucatan Channel respectively (Fig. 1).

The location of the LC front is determined here using a methodology that locates the LC fronts and detects the shedding of LC rings based on the maximum horizontal gradient of sea surface height (SSH) with a spatial resolution of 0.25 degree and a temporal resolution of one week (e.g., Lindo-Atichati et al., 2013). Specifically, the northernmost and westernmost locations of the LC are detected from the maximum latitude and longitude of the SSH contours corresponding to the location of the maximum gradient of SSH (Fig. 2). This methodology is based on a technique previously developed to investigate the link between GoM mesoscale features and larval fish distribution (Lindo-Atichati et al., 2012).

Continuous wavelet transforms (CWT) of the time series presented here are used to analyze the variability of the dominant periods of the series, and a wavelet-based semblance analysis is used to correlate them. Semblance analysis allows the local phase relationships between the two datasets to be studied as a function of both scale (or wavelength) and time (Cooper and Cowan, 2008).

3 Results

Time series of monthly LC migrations anomalies (LCMA) and monthly atmospheric boundary-layer SLPG are computed for 20 years of data, from January 1993 to December 2012 (Fig. 3). LCMA are defined here as the difference between the mean northernmost latitudes of LC front for each specific month [°N] and that for the same month since November 1992. SLPG is defined here as the difference between the monthly atmospheric boundary-layer sea level pressure in the northernmost location of the LC [mb] and that of the southernmost location of the LC. A close inspection of Fig. 3 qualitatively reveals that LC meridional migrations and the SLPG are anti-correlated being out of phase ($r = -0.53$; $p = 0.03$). This is indicative that when the atmospheric pressure meridional gradient increases the LC retreats southward. Conversely, when it

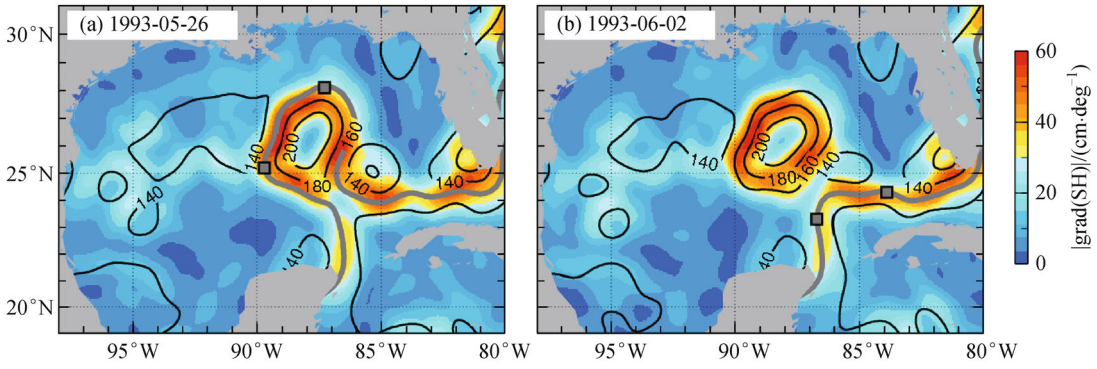

Fig. 2 Fields of altimetry-derived Sea Surface Height gradient [cm·deg^{-1}] and Sea Surface Height contours [cm] in the Gulf of Mexico (GoM). Fields illustrate the detected LC front (grey contour) when the LC is located in (a) the northern and (b) the southern GoM. The northernmost and westernmost locations of the LC front are tagged with a square in both panels.

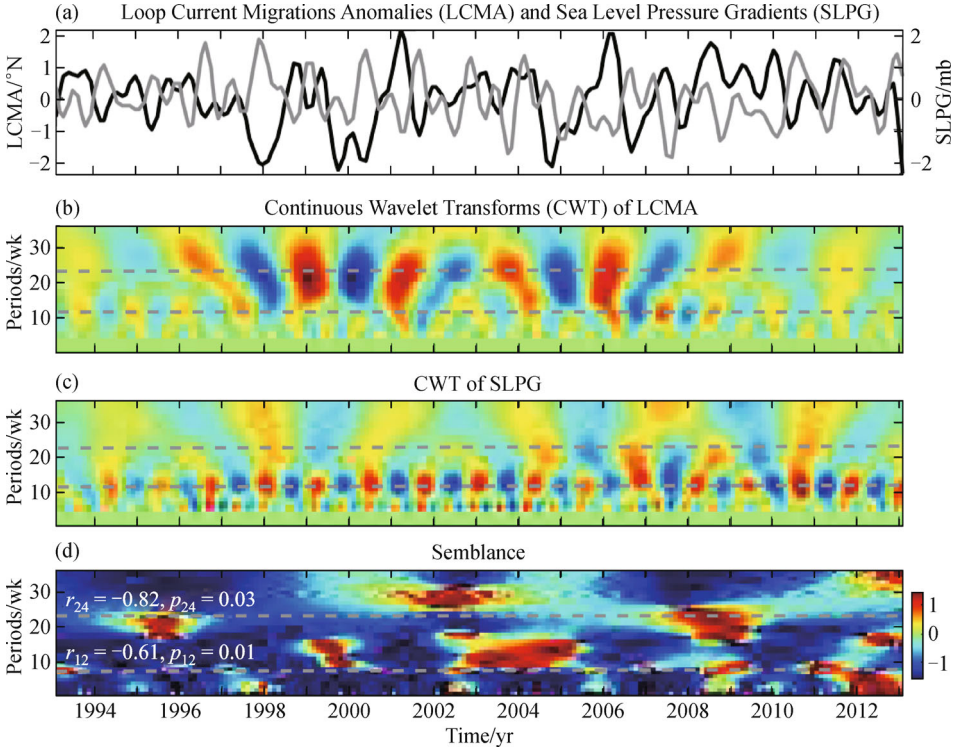

Fig. 3 (a) Time series of monthly Loop Current Migration Anomalies (LCMA, black curve) and time series of monthly Sea Level Pressure Gradient (SLPG, grey curve) determined from the pressure difference between the mean northernmost and southernmost locations of the Loop Current front, from January 1993 to December 2012. (b) Real part of the complex Continuous Wavelet Transform (CWT) of LCMA time series. Bright red indicates large positive amplitude and dark blue indicates large negative amplitude. (c) Real part of the complex CWT of SLPG time series. Bright red indicates large positive amplitude and dark blue indicates large negative amplitude. (d) Semblance index, S. Bright red corresponds to a positive semblance and dark blue to a negative semblance. Wavelength ranges from zero to 36 weeks. Grey dashed lines highlight the periods of 12 weeks and 24 weeks, which are clear examples of periods with significant moderate to strong negative correlations.

decreases the LC intrudes northward. For example, the LC migrated north from January 1998 to September 1998, then moved south from October 1998 to January 1999, and finally started another northward intrusion from February 1999 to April 1999. For the same period — from January 1998 to April 1999 — SLPG described an antiphase oscillation to that described by the LC, decreasing SLPG when the LC migrated northward and increasing SLPG when the LC retreated southward. In general we may qualitatively appreciate that this anticorrelation holds for all the analyzed period, although it fails in 2005, 2011, and 2012 (Fig. 3). Continuous wavelet transforms of LCMA

time series point out that the variability is dominated by high amplitude 24 weeks (i.e., semiannual) periods and low amplitude 12 weeks (Fig. 3(b)) periods. Similarly, there is also a clearly periodicity of 24 weeks for SLPG time series, although this signal is faded by a higher amplitude at 12 weeks period (Fig. 3(c)). Semblance analysis between two series quantitatively shows an anti-correlation higher than 75% for both periods along the 80% of our time domain. For example, LCMA and SLPG show a moderate significant anticorrelation at 12 weeks period ($r = -0.61$; $p = 0.01$) and a strong significant anticorrelation at 24 weeks period ($r = -0.83$; $p = 0.02$).

Because wind stress variability drives Ekman transport (Cunningham et al., 2007), the anticorrelation between meridional SLPG and LC migrations may be an indication that the mechanism that may force LC migration is linked with the zonal wind intensity. We explore the variability of meridional gradient of zonal wind stress (WSG). WSG is defined as the difference between the monthly zonal (east-west) wind stress in the northernmost location of the LC [$N \cdot m^{-2}$] and that of the southernmost location of the LC. As expected, time series of mean zonal WSG and time series of SLPG correlate and they are in phase (Fig. 3(a) and 4(a)). Therefore, time series of the WSG and time series of LC migration are out of phase as shown by Fig. 4(a). Analogously to the case of SLPG, there are also periodicities of 12 weeks for the time series of WSG (Fig. 4(c)). The semblance analysis showed a negative correlation at all periods along most of the time interval (blue regions on Fig. 4(d)). In particular the negative correlation between the LC migrations and the wind stress is higher than 80% at time scales of 20±4 weeks (mean±SD). For example, LCMA and WSG show a moderate significant anticorrelation at 12 weeks period ($r = -0.57$; $p = 0.02$) and a moderate marginally significant anticorrelation at 24 weeks period ($r = -0.68$; $p = 0.09$).

4 Discussion and conclusions

The above results suggest that LC variability is significantly modulated to some extent by the meridional atmospheric pressure gradient and thus by the related mean westward wind stress linked to the variability of trade winds. These results complement some of the many efforts that have been made in the past to describe the processes and the mechanisms of the LC intrusions and the shedding of LC rings in the GoM.

Regarding the processes, most of the descriptions connected the LC intrusions and LC ring formations with the transport through the Yucatan Channel (Maul et al., 1985; Oey, 1996; Bunge et al., 2002; Candela et al., 2003;

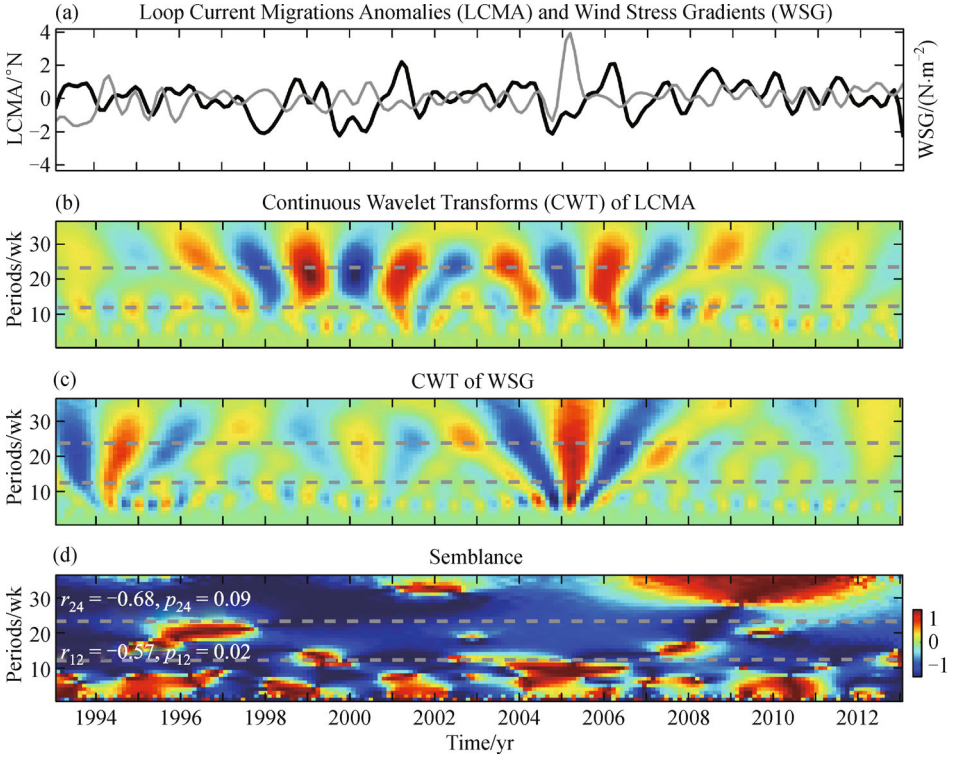

Fig. 4 (a) Time series of monthly Loop Current Migration Anomalies (LCMA) and time series of the monthly Wind Stress Gradient (WSG) averaged between northernmost and southernmost locations Loop Current, from January 1993 to December 2012. (b) Real part of the complex Continuous Wavelet Transform (CWT) of the LCMA time series. (c) Real part of the complex CWT of the WSG time series. (d) Semblance index, S. Grey dashed lines highlight the periods of 12 weeks and 24 weeks, which are clear examples of periods with significant moderate to strong negative correlations.

Ezer et al., 2003; Chérubin et al., 2005). The growth of the LC as it expands to the north displaces an approximately equivalent volume of Gulf water, which is observed to flow back into the Caribbean Sea at depths below 800 m (Bunge et al., 2002). Further, the LC shows cyclonic eddies around its edge, which may grow as they propagate around its periphery and are sometimes linked to the separation of the LC into the LC rings (Fratantoni et al., 1998). The LC rings typically drift toward the west or west-northwest and reach the Texas-Mexico coastal zone after 2−4 months (Müller-Karger et al., 1991). Immediately after shedding a ring, the LC retracts to a southern position, where waters flow more directly between Yucatan Strait and the Straits of Florida. Therefore, it should also be considered that the major retreatment of the LC is associated with the detachment of anticyclonic LC rings. The process of LC extension and ring separation is often stochastic (Nowlin et al., 2000; Zavala-Hidalgo et al., 2006). However, after 20 years of altimeter-derived observations, the northward extension of the LC and detachments of LC rings show some seasonal preferences in the timing of these events (Alvera-Azcárate et al., 2009; Lindo-Atichati et al., 2013), which is consistent with similar modeling results (Chang and Oey, 2012). With this work we shed some light on these processes by providing observational evidences to the argument that these seasonal preferences might be linked to the seasonal variability of the prevailing zonal wind field in the region. Specifically, we provided observational evidences that positive (negative) WSG of the prevailing zonal wind may trigger LC migrations to the south (north) at time scales of 3 months and 6 months. Similarly, the intensification and weakening of the Caribbean Current has been recently been linked to the seasonal variability of the Trade Winds and North Atlantic Current (Nedbor-Gross et al., 2014).

Regarding the mechanisms, many studies have demonstrated that physical properties of the water masses of the upper GoM (e.g., Sea Surface Temperature) are determined by interaction of the ocean and the atmosphere over seasonal cycles (Vidal et al., 1994; Herring, 2010 and references therein). Along the GoM shelves, wind forcing drives most of the variability and the along-coast wind stress is highly correlated with the local currents (Cho et al., 1998; Nowlin et al., 1998; Zavala-Hidalgo et al., 2003; Walker et al., 2005). In the central and deep portion of the basin, the variability of the anticyclonic circulation is driven by a combination of wind stress and LC rings (Sturges et al., 1993; Nowlin et al., 2000; Lee and Mellor, 2003; DeHaan and Sturges, 2005). Using numerical experiments with and without atmospheric forcing, Chang and Oey (2010) were the first to propose a mechanism that explains the delay in the detachment of rings and the formation of larger rings. In this mechanism, the wind produces westward transports over the northern and southern shelves of the Gulf, convergence in the west, and a returned eastward upper-layer flow over the deep central basin toward the LC. However, more evidences are needed to say that wind drives the westward transport. The 'momentum imbalance paradox' theory (Pichevin and Nof, 1997; Nof, 2005) is used to explain that this returned flow constitutes a zonal momentum flux that delays ring shedding, and also that this wind-generated returned flow forces larger LC and rings. Our observational results support the idea that the wind stress variability is related with the LC intrusions variability. Although the entire cycle of the LC expansion, ring shedding, and LC retraction is a highly nonlinear process (Le Hénaff et al., 2012), ring shedding and LC migrations are closely related by means of the Yucatan Transport (Xu et al., 2013). Nof (2005) shows that a growing ring detaches when it reaches a size where the Rossby radius is greater than the growth rate of the LC because of inflow from the Yucatan Channel (i.e., the Yucatan Transport). The key point here is that the returned flow originated by the wind counteracts the westward Rossby wave speed. This tends to force the LC to grow to a larger size before it sheds the LC ring, prolonging the shedding period as well as making the ring larger. Consequently, more mass is accumulated in the LC and rings, and likely more mass exchange is produced between the Gulf and the Caribbean Sea via the Yucatan Channel. Our results based on a 20 years analysis of altimetry data show evidences that the weakening in the wind stress in the eastern GoM is related with the LC intrusions to the north. The weakening of the wind stress — i.e., negative WSG — and LC intrusions might also be associated with an increase in the Yucatan Transport, which would balance the increase in the westward Rossby wave speed of a growing loop and ultimately delay the shedding of LC rings. This is consistent with recent finding that show that drops in the Caribbean wind stress produce decrease in the Yucatan Transport, because in the GoM the seasonal zonal wind is 180° out of phase with the Caribbean wind (Chang and Oey, 2013b).

The links between the YC transport and the LC variability, LC ring shedding, and the overall dynamics in the GoM have been further investigated in a number of studies (Ezer et al., 2003; Oey 2004; Lin et al., 2009; Chang and Oey, 2011; Le Hénaff et al., 2012). In those papers, the model setup always includes some combination of boundary conditions and atmospheric forcing. The authors conclude that the LC variability (expansion, retraction and shedding) is correlated with the flow conditions in the YC. They found a correlation in the expansion of the LC and in the deep return flow below 800 m at the YC. Also, they conclude that while vorticity and transport fluctuations at the YC may explain the irregular ring shedding, the LC behavior cannot be wholly explained in terms of YC flow conditions. However, Lin et al. (2009) studied the variation in the vertically integrated YC transport that accompanies LC intrusion and ring shedding. They view these transport variations as a consequence of LC intrusion rather than the cause of the

LC intrusion itself, and shown that the YC transport reaches a minimum when the LC intrusion into the GoM is maximum, typically just prior to ring shedding. Likewise, the maximum YC transport occurs typically soon after a ring has been shed and is partly compensated by flow around Cuba. Numerical simulations showed two mechanisms for YC transport variations associated with the LC intrusion: 1) at time scales longer than 30 days, the mechanism driving this compensation effect is the interaction between the density anomalies associated with Loop Current intrusion and the variable bottom topography, with a formation of a drag effect across the ridge connecting Florida and Cuba; and 2) at time scales shorter than 30 days, the dynamics driving this compensation effect are wind driven. We showed time series that indicate that WSG and LC migration variability are out of phase at 12 and 24 weeks. These observational results do not support mechanism 2) from Lin et al. (2009). However, the monthly nature or our data does not allow corroborating Lin at al. (2009) at time scales shorter than 30 days.

The comprehensive modeling work by Cardona and Bracco (2014) showed that the LC behavior is governed by a component forced by the YC transport strength, atmospheric forcing, and bathymetry constrains. Transport and vorticity fluctuations in the YC, together with the wind forcing, contribute to the ring detachment, but while a preferred tendency for LC shedding can be found for specific conditions of all three, authors did not find these to be sufficient predictors. Probably because our time series covers longer time scales, we are able to show observational evidences that the atmospheric forcing may be a significant component for governing the LC behavior. Much of those models would benefit of using high frequency atmospheric forcing instead of monthly atmospheric forcing. High resolution atmospheric forcing is likely to change dramatically the representation of vertical mixing by exciting quasi-inertial waves as ageostrophic expression of the mesoscale eddy field.

Noteworthy, our investigation of the atmospheric modulation of the LC has been conducted regionally, i.e., in the region of the GoM occupied by the LC during its excursions. The wind field in the entire Caribbean Sea produces transport variability in the Yucatan Channel, and Nedbor-Gross et al. (2014) also suggested that there is a relationship between the Yucatan channel deep transport and the LC area. However, what is the independent contribution of the Yucatan transport to the LC excursions is still unknown and must be investigated in future studies.

The apparent anticorrelation between the LC migrations and the monthly wind stress anomalies present some exceptions during 2005, 2011, and 2012. The eastern Gulf of Mexico experienced hurricane seasons that were significantly more active during 2005, 2011, and 2012 in terms of total number of tropical depressions, tropical storms, and hurricanes (ANOVA: $p < 0.01$). Therefore, it is likely that the sudden high wind fields associated with the very active tropical seasons were not mirrored on LC migrations during these years.

In summary, the Loop Current migrations and ring shedding events receive much attention because these two powerful oceanic features carry anomalies in the physical, biological, and chemical properties that affect just about every aspect of oceanography of the Gulf. To date, we have a 20 years record of satellite altimetry observations of variations in ocean surface topography. This long-term availability of satellite altimetry data allows analyzing the mesoscale eddy variability and the fundamental processes controlling geostrophic ocean currents. We show for the first time observational evidences of an atmospheric modulation of the Loop Current migrations, which are anticorrelated with the atmospheric boundary-layer sea level pressure and with the predominantly zonal wind stress regime. We therefore provide a baseline against which current ocean models can explore the dynamical mechanisms for this observed anticorrelation.

Although the LC intrusion and detachment of rings is commonly accepted to be a chaotic process, our observations give room to think that LC intrusions might occur under certain wind direction and stress.

Acknowledgements The altimeter products were produced by Ssalto/Duacs (Segment sol multimissions d'Altimétrie, d'Orbitographie et de localisation précise/Developing Use of Altimetry for Climate Studies) and distributed by AVISO, with support from Centre National d'Etudes Spatiales (CNES). The authors are grateful to Lie-Yauw Oey from Princeton University and two anonymous reviewers for providing suggestions and comments that have improved the article. This work was supported by NOAA/AOML.

References

Alvera-Azcárate A, Barth A, Weisberg R H (2009). The surface circulation of the Caribbean Sea and the Gulf of Mexico as inferred from satellite altimetry. J Phys Oceanogr, 39(3): 640–657

Bunge L, Ochoa J, Badan A, Candela J, Sheinbaum J (2002). Deep flows in the Yucatan Channel and their relation to changes in the Loop Current extension. J Geophys Res, 107(C12): 3233

Candela J, Tanahara S, Crepon M, Barnier B, Sheinbaum J (2003). Yucatan Channel flow: observations versus CLIPPER ATL6 and MERCATOR PAM models. J Geophys Res, 108(C12): 3385

Cardona Y, Bracco A (2014). Predictability of mesoscale circulation throughout the water column in the Gulf of Mexico. Deep Sea Res Part II Top Stud Oceanogr, doi: 10.1016/j.dsr2.2014.01.008

Chang Y L, Oey L Y (2010). Why can wind delay the shedding of Loop Current eddies? J Phys Oceanogr, 40(11): 2481–2495

Chang Y L, Oey L Y (2011). Loop Current cycle: coupled response of the Loop Current with deep flows. J Phys Oceanogr, 41(3): 458–471

Chang Y L, Oey L Y (2012). Why does the Loop Current tend to shed more eddies in summer and winter? Geophys Res Lett, 39(5): n/a doi: 10.1029/2011GL050773

Chang Y L, Oey L Y (2013a). Loop Current growth and eddy shedding using models and observations: numerical process experiments and satellite altimetry data. J Phys Oceanogr, 43(3): 669–689

Chang Y L, Oey L Y (2013b). Coupled response of the trade wind, SST gradient, and SST in the Caribbean Sea. J Phys Oceanogr, 43(7): 1325–1344

Chérubin L M, Sturges W, Chassignet E P (2005). Deep flow variability in the vicinity of the Yucatan Straits from a high-resolution numerical simulation. J Geophys Res, 110(C4): C04009

Cho K, Reid R O, Nowlin W D Jr (1998). Objectively mapped stream function fields on the Texas-Louisiana shelf based on 32 months of moored current meter data. J Geophys Res, 103(C5): 10377–10390

Clancy R M (1992). Operational modeling: ocean modeling at the Fleet Numerical Oceanography Center. Oceanography (Wash DC), 5(1): 31–35

Cooper G R J, Cowan D R (2008). Comparing time series using wavelet-based semblance analysis. Comput Geosci, 34(2): 95–102

Cunningham S A, Kanzow T, Rayner D, Baringer M O, Johns W E, Marotzke J, Longworth H R, Grant E M, Hirschi J J M, Beal L, Meinen C S, Bryden H L (2007). Temporal variability of the Atlantic meridional overturning circulation at 26.5 N. Science, 317(5840): 935–938

DeHaan C J, Sturges W (2005). Deep cyclonic circulation in the Gulf of Mexico. J Phys Oceanogr, 35(10): 1801–1812

Ezer T, Oey L Y, Lee H C, Sturges W (2003). The variability of currents in the Yucatan Channel: analysis of results from a numerical ocean model. J Geophys Res, 108(C1): 3012

Fratantoni P S, Lee T N, Podesta G P, Muller-Karger F (1998). The influence of Loop Current perturbations on the formation and evolution of Tortugas eddies in the southern Straits of Florida. J Geophys Res, 103(C11): 24759

Herring J H (2010). Gulf of Mexico hydrographic climatology and method of synthesizing subsurface profiles from the satellite sea surface height anomaly. US. Department of Commerce, National Oceanic and Atmospheric Administration. National Ocean Service, Coastal Survey Development Laboratory. Report 122. 63 pp

Hurlburt H, Thompson J D (1980). A Numerical Study of Loop Current Intrusions and Eddy Shedding. J Phys Oceanogr, 10(10): 1611–1651

Le Hénaff M, Kourafalou V H, Morel Y, Srinivasan A (2012). Simulating the dynamics and intensification of cyclonic Loop Current Frontal Eddies in the Gulf of Mexico. J Geophys Res, 117 (C2): C02034

Lee H C, Mellor G L (2003). Numerical simulation of the Gulf Stream System: the Loop Current and the deep circulation. J Geophys Res, 108(C2): 3043

Lin Y, Greatbatch R J, Sheng J (2009). A model study of the vertically integrated transport variability through the Yucatan Channel: role of Loop Current evolution and flow compensation around Cuba. J Geophys Res, 114(C8): C08003

Lindo-Atichati D, Bringas F, Goni G (2013). Loop Current excursions and ring detachments during 1993–2009. Int J Remote Sens, 34(14): 5042–5053

Lindo-Atichati D, Bringas F, Goni G, Muhling B, Muller-Karger F E, Habtes S (2012). Varying mesoscale structures influence larval fish distribution in the northern gulf of Mexico. Mar Ecol Prog Ser, 463: 245–257

Maul G A, Mayer D A, Baig S R (1985). Comparisons between a continuous 3-year current-meter observation at the sill of the Yucatan Strait, satellite measurements of Gulf Loop Current area, and regional sea level. J Geophys Res, 90(C5): 9089–9096

Muller-Karger F E, Smith J P, Werner S, Chen R, Roffer M, Liu Y, Muhling B A, Lindo-Atichati D, Lamkin J, Cerdeira-Estrada S, Enfield D B (2014). Natural variability of surface oceanographic conditions in the offshore Gulf of Mexico. Prog Oceanogr, 134: 54–76

Müller-Karger F E, Walsh J J, Evans R H, Meyers M B (1991). On the seasonal phytoplankton concentration and sea surface temperature cycles of the Gulf of Mexico as determined by satellites. J Geophys Res, 96(C7): 12645–12665

Muñoz E, Busalacchi A J, Nigam S, Ruiz-Barradas A (2008). Winter and summer structure of the Caribbean low-level jet. J Clim, 21(6): 1260–1276

Nedbor-Gross R, Dukhovskoy D S, Bourassa M A, Morey S M, Chassignet E P (2014). Investigation of the relationship between the Yucatan Channel transport and the Loop Current area in a multidecadal numerical simulation. Mar Technol Soc J, 48(4): 15–26

Nof D (2005). The momentum imbalance paradox revisited. J Phys Oceanogr, 35(10): 1928–1939

Nowlin W D, Jochens A E, DiMarco S F, Reid R O (2000). Physical oceanography. Deepwater Gulf of Mexico environmental and socioeconomic data search and synthesis, Narrative Report, OCS Study MMS 2000-049,Gulf of Mexico OCS Regional Office, Minerals Management Service, U.S. Department of the Interior 1, 60

Nowlin W D, Jochens A E, Reid R O, DiMarco S F (1998). Texas-Louisiana Shelf Circulation and Transport Processes Study: Synthesis Report. Volume I: Technical Report. OCS Study MIMS 98-0035, U.S. Department of the Interior, Minerals Management Service, Gulf of Mexico OCS Region, 502 pp

Oey L Y (1996). Simulation of mesoscale variability in the Gulf of Mexico: sensitivity studies, comparison with observations, and trapped wave propagation. J Phys Oceanogr, 26(2): 145–175

Oey L Y (2004). Vorticity flux through the Yucatan Channel and Loop Current variability in the Gulf of Mexico. J Geophys Res, 109(C10): C10004

Pichevin T, Nof D (1997). The momentum imbalance paradox. Tellus, Ser A, Dyn Meterol Oceanogr, 49(2): 298–319

Poveda G, Waylen P R, Pulwarty R S (2006). Annual and inter-annual variability of the present climate in northern South America and southern Mesoamerica. Palaeogeogr Palaeoclimatol Palaeoecol, 234 (1): 3–27

Smith R H, Johns E M, Goni G J, Trinanes J, Lumpkin R, Wood A M, Kelble C R, Cummings S R, Lamkin J T, Privoznik S (2014). Oceanographic conditions in the Gulf of Mexico in July 2010, during the Deepwater Horizon oil spill. Cont Shelf Res, 77: 118–131

Sturges W, Evans J C, Welsh S, Holland W (1993). Separation of warm-core rings in the Gulf of Mexico. J Phys Oceanogr, 23(2): 250–268

Tomczak M, Godfrey J S (2003). Regional Oceanography: An Introduction. Oxford: Pergamon

Vidal V M V, Vidal F V, Hernández A F, Meza E, Zambrano L (1994). Winter water mass distributions in the western Gulf of Mexico affected by a colliding anticyclonic ring. J Oceanogr, 50(5): 559–588

Walker N D, Wiseman W J Jr, Rouse L J Jr, Babin A (2005). Effects of river discharge, wind stress, and slope eddies on circulation and the satellite-observed structure of the Mississippi River plume. J Coast Res, 216(6): 1228–1244

Wang C (2007). Variability of the Caribbean low-level jet and its relations to climate. Clim Dyn, 29(4): 411–422

Wang C, Lee S (2007). Atlantic warm pool, Caribbean low-level jet, and their potential impact on Atlantic hurricanes. Geophys Res Lett, 34 (2):L0 2703

Xu F H, Chang Y L, Oey L Y, Hamilton P (2013). Loop Current growth and eddy shedding using models and observations: analyses of the July 2011 Eddy-Shedding Event*. J Phys Oceanogr, 43(5): 1015–1027

Zavala-Hidalgo J, Morey S L, O'Brien J J, Zambudio L (2006). On the Loop Current eddy shedding variability. Atmosfera, 19(001): 8

Zavala-Hidalgo J, Morey S L, O'Brien J J (2003). Seasonal circulation on the western shelf of the Gulf of Mexico using a high-resolution numerical model. J Geophys Res, 108(C12): 3389